UCRL - 74664
PREPRINT

LAWRENCE LIVERMORE LABORATORY
University of California/Livermore, California

DYNAMIC PIEZORESISTIVITY OF MANGANIN TRANSDUCERS

James W. Lyle
David L. Banner
Roger L. Brier

April 1973

This paper was prepared for submission to the
Journal of Applied Physics

DYNAMIC PIEZORESISTIVITY OF MANGANIN TRANSDUCERS*

J. W. Lyle, D. L. Banner, and R. L. Brier

Lawrence Livermore Laboratory, University of California
Livermore, California

ABSTRACT

Manganin, an alloy of copper, manganese and nickel, has been used as a dynamic piezoresistive transducer for shock wave profile measurement in the range from 22 to 410 kbar. Thirty-six gun-accelerated flyer plate impact experiments were performed to dynamically calibrate wires of 1 mil diameter that were electricically insulated with thin dielectric sheets and cemented between target plates. A static calibration gave a linear, reversible, pressure derivative of 2.5 ± 0.1 Ω/Ω/Mbar to 90 kbar. The dynamic calibration is linear within ±5% to 200 kbar with a pressure derivative of 2.7 ± 0.1 Ω/Ω/Mbar. At stresses higher than 200 kbar, the dynamic response becomes slightly nonlinear and the data were fit with the polynomial expression:

$$\sigma = 0.3896(\Delta R/R) - 0.2348(\Delta R/R)^2 + 0.5825(\Delta R/R)^3 - 0.3360(\Delta R/R)^4,$$

with a standard deviation of ±4.4 kbar where the stress σ is in megabar. A linear hysteresis was observed with a pressure derivative of 2.6 ± 0.1 Ω/Ω/Mbar during unloading from a peak stress in the range from zero to 247 kbar.

INTRODUCTION

The linear piezoresistive property of Manganin alloy has made it a favorite electrical transducer for static high pressure measurement for the past seventy years. Its dynamic response to shock-induced stresses was first investigated by Fuller and Price[1] in the early 1960's and later by Keough and Wong[2] and by Barsis et al.[3] Various alloy compositions were used and comparisons were made between the alloy in wire and foil form in a great variety of insulator configurations. A fair amount of scatter exists in the data, and it was recognized that the dynamic calibration may be nonlinear, and that the gauge displays hysteresis. This article contains the results of 36 experiments to measure the dynamic response of in-situ gauges in the stress range from 22 to 410 kbar, and the results of 7 experiments to measure hysteresis from zero to 247 kbar.

The alloy was used in wire form and cemented with thin dielectric sheets between metal or ceramic discs. Shock waves were driven into the assemblies by the flat impact of gun-accelerated flyer plates.

The in-situ Manganin gauge causes a disturbance, in the propagation of stress waves, proportional to its thickness and the relative shock impedances of gauge and target. In most of our work, the impedances of the targets were three to six times that of the gauge. The resulting stress and rarefaction wave reflections at the gauge boundaries cause a loss of the higher frequency components of the transmitted wave in the target and produce, by interactions with waves from free surfaces and other interfaces, a variety of effects including internal spall and the opening and closing of voids at surfaces of no strength.

The one-dimensional hydrodynamic finite difference computer calculation described by Wilkins[4] was used to interpret the gauge response. Included in the problem statement are the equations of state (EOS) and constitutive relations of flyer, gauge, and target materials listed in Appendix A. These were obtained by reference to the literature and by experiments with the gauge to obtain its own EOS.

The dynamic resistance change of the gauge was monitored by cathode ray tube oscilloscopes. It was observed that the signal failed to return to baseline upon unloading from a peak stress to zero stress. An experiment was designed in which the stress was reduced in steps by multiple wave reflections in the flyer plate. The resulting record displayed hysteresis when compared to a machine calculation of the wave profile. The calculation was verified in a comparison experiment in which the particle velocity was measured using the electromagnetic technique of Zaitsev.[5]

EXPERIMENTAL TECHNIQUE

The Manganin wire that was used in these experiments was drawn by the California Fine Wire Company[6] to 1-mil diam, from 10-mil diam precision grade stock obtained from the Wilbur B. Driver Company. After the final draw the wire was stress-relieved at 485°C in a hydrogen atmosphere. The composition, determined by wet chemistry, was 12.95 wt% Mn, 4.28 wt% Ni, and the balance, Cu and impurities. The impurities quoted by the supplier are: 0.32% Fe and 0.01% Si, which are

introduced during drawing. The lattice symmetry is face-centered cubic with a constant of 3.66 Å. Specific resistivity of the wire is 48.1 ± 0.4 $\mu\Omega$cm.

Gauges were made of bare Manganin wires by electroplating 10 cm bands of copper onto both ends. The bare portion in the middle was approximately 1 cm long, with a resistance between 7 and 10 Ω. The copper leads had handbook-value specific resistivity, and comprised less than 2% of the total gauge resistance. The plated ends of the wires were flattened in a hydraulic press to about 1 mil thick; the Manganin portion remained circular. This method of gauge construction minimizes the capacitance-to-metal shot parts and, because of the low resistance, eliminates the negative-going precursor signal often observed with higher-resistance photo-etched foil gauges.

The plated wires were assembled as a two-terminal transducer between sheets of mica[7] or sheets of Kapton[8] using epoxy[9] resin as an adhesive. The dielectric sheets were from 1 to 3 mil thick, and the total gauge thickness ranged from 3 to 7 mil. Kapton is the preferred insulator at stresses less than 0.2 Mbar because the electrical signals are less noisy than with mica. Mica is preferred at stresses greater than 0.2 Mbar because it is stiffer than Kapton and the gauges last longer before electrical shorting to metallic shot parts. In nearly all the measurements with mica-insulated gauges in metals, the elastic precursors, if present, were obscured in the initial electrical noise thought to be caused by the compression of the laminar mica.

The gauges were cemented with epoxy between discs of metal or ceramic and placed in an evacuated chamber before the muzzle of a gun. In

the case of metals shocked beyond 0.2 Mbar, it was found useful to machine cylindrical surfaces of radius 12.7 cm on the mating target parts at the gauge location to delay lead failure for several microseconds after the signal. This is shown in Fig. 1. Shocks in the targets were generated by the flat impact of flyer plates of the same material. Our procedures in gun technique for accelerating the flyer plates closely follow those described by Thunborg.[10]

In all experiments the release rarefaction originated at the rear surface of the flyer. At the lower impact velocities the flyer was supported only at the rim; the release was to zero stress, and thus useful as a measure of gauge hysteresis. At the higher velocities the flyers were supported by carbon foam (ρ_o = 0.4 gm/cm), polymethylmethacrylate (PMMA), or epoxy resin.

A simplified circuit diagram is shown in Fig. 2. A charged capacitor voltage source supplies a square pulse through the closure of switches, S_1 and S_2, to the resistive isolation networks, and thence to a bridge consisting of the gauge, a balance resistor, and the amplifiers contained in a differential preamplifier oscilloscope. Calibration is accomplished by comparison to a record made by substituting several standard resistors at the gauge location.

RESULTS

The dynamic calibration data are listed in Table I. In addition, a quasihydrostatic measurement of the wire gave a pressure derivative of

2.5 ± 0.1 Ω/Ω/Mbar, which compares with 2.42 Ω/Ω/Mbar reported by Barsis.[3] The data in the pressure range up to 100 kbar is plotted in Fig. 3 to illustrate the scatter and the relation to the static determination. A least squares linear fit to the data up to 200 kbar gave a pressure derivative of 2.7 ± 0.1 Ω/Ω/Mbar. At stresses higher than 200 kbar there is a gradual decrease in the pressure derivative until the region near 400 kbar is approached, where the derivative increases again. All the data were fit with a least squares fourth-order polynomial:

$$\sigma = 0.3896\,(\Delta R/R) - 0.2348\,(\Delta R/R)^2 + 0.5825\,(\Delta R/R)^3 - 0.3360\,(\Delta R/R)^4 \pm 0.0044 \text{ Mbar standard deviation.}$$

A pair of experiments was conducted to observe points along the release path in PMMA from a maximum stress of 31 kbar. The first of these employed an electromagnetic detector of particle velocity according to the technique described by Zaitsev[5] and by Al'tshuler.[11] The second contained Manganin gauges and shows the characteristic hysteresis behavior. The geometry for these experiments is described for Shot 3226 in Table II, and Fig. 4 is a distance vs time plot that illustrates the multiple wave reflections in the flyer plate that produce the stepped release in the PMMA. Figures 5 and 6 show the experimental results and the computer calculations. The purpose of the particle velocity measurement was to verify the calculation along the release using the EOS and constitutive relations for PMMA that are found in Appendix A. The empirical observation was made that the hysteresis of Manganin is linear with the decrease in stress, and

that the release path can be fit with an equation of the form:

$$\sigma = \sigma_1 - (0.38 \pm 0.01) \frac{R_1 - R}{R_0}$$

where σ is the released stress, σ_1 is maximum stress, R_1 is the resistance at σ_1, R_0 is the initial resistance. This equation was used to calculate release stresses in six other experiments in the range up to 247 kbar with a maximum error of 6.7%. The data appear in Table II.

DISCUSSION

The accuracy of the results reported here is limited by uncertainties in flyer velocities (which were measured to within 1%), and in equations-of-state and constitutive relations for materials that were shocked to stresses above their Hugoniot elastic limits. In addition, "identical" gauges in the same experiment often exhibit variations of several percent in $\Delta R/R_0$. Therefore, stresses calculated from the gauge performance listed here are only considered accurate to within ±5%.

At present, there is no generally recognized explanation for the piezoresistive behavior of Manganin which would allow one to quantitatively or qualitatively predict the observed increase in resistance with increasing stress, or to predict the magnitude of the hysteresis. Rosenberg[12] pointed out that the piezoresistance coefficient of Manganin was decreased by prior cold work. Similarly, Keough[2] suggested that shear deformation causes

lattice defect generation and accounts for the greater observed resistivity change of wires compared to foils in the same one-dimensional shock environment. If lattice defects cause the hysteresis, then suitable prior cold working treatment may make possible Manganin gauges with wide range linear response without hysteresis.

APPENDIX A

Equations of State and Constitutive Relations of Materials Used to Calibrate Manganin Gauges

Symbol	Definition	Unit
ρ_0	Initial density	gm/cm^3
C_ℓ	Longitudinal sound speed	$cm/\mu sec$
σ	Stress	Mbar
U_P	Particle velocity	$cm/\mu sec$
$V_0 = \frac{1}{\rho_0}$	Initial specific volume	cm^3/gm
V	Specific volume	cm^3/gm
$\mu = \frac{V_0}{V} - 1$	Compression	dimensionless
HEL	Hugoniot elastic limit	kbar
Y_0	Yield strength	kbar
G	Shear modulus	kbar
E	Energy/initial volume	Mbar - cm^3/cm_0^3
P	Pressure	Mbar

1. Alumina, Diamonite, P-3142-1, Diamonite Products Co., Shreve, Ohio.[13] Used in its elastic range only.

$\rho_0 = 3.72$ $\quad C_\ell = 0.99$ $\quad$ HEL = 88 ± 5 kbar

$\sigma = 1.902\,\mu + 0.1521\,\mu^2$

2. Aluminum alloy 2024-T4[14,15]

$\rho_0 = 2.785$ $\quad Y_0 = 2.8$ kbar $\quad G = 287$

$P = 0.73\,\mu + 1.72\,\mu^2 + 0.4\,\mu^3$

3. Aluminum alloy 6061-T6[15,16]

$\rho_0 = 2.70$ $\quad Y_0 = 3$ kbar $\quad G = 248$ kbar

$P = 0.73\,\mu + 1.72\,\mu^2 + 0.4\,\mu^3$

4. Uranium[17]

$\rho_0 = 19.045$ $\quad Y_0 = 12$ kbar $\quad G = 844$ kbar

$$P = \frac{1.171\,\mu\,(1 - 0.21\mu - 0.295\,\mu^2)}{(1 - 0.53\,\mu)^2} + (2.42 + 0.59\,\mu)\,E$$

5. Sapphire, single crystal Z-cut Al_2O_3.[18] Used in its elastic range only.

$\rho_0 = 3.985$ $\quad C_\ell = 1.119$ $\quad$ HEL > 120 kbar

$\sigma = \rho_0 (1.119 + 1.\ U_P) U_P$

6. Copper, OFHC[19]

$\rho_0 = 8.93$ $Y_0 = 1.2$ kbar $G = 477$ kbar

$P = 1.19\,\mu + 4.435\,\mu^2$

7. Magnesium alloy AZ31B[20]

$\rho_0 = 1.735$ $Y_0 = 1.7$ kbar $G = 165$ kbar

$P = 0.37\,\mu + 0.54\,\mu^2 + 0.186\,\mu^3$

8. PMMA, Polymethylmethacrylate[18]

$\rho_0 = 1.185$ $Y_0 = 1.5 \exp\left(-\frac{E \times 10^{-16}}{0.0058 - E}\right)$ kbar $G = 23.2$ kbar

$$P = \frac{0.0593\,\mu\,(1 + 0.575\,\mu)}{\left(1 - 1.088\,\mu + 1.124\,\frac{\mu^2}{\mu + 1}\right)^2} + 0.85\,E$$

9. Silica, Dynasil 1000.[18] Used in the nonlinear elastic range only.

$\rho_0 = 2.201$

$\sigma = 0.7745\,\mu - 4.404\,\mu^2 + 30.15\,\mu^3 - 70.37\,\mu^4 + 0.0752\,E$

10. Alumina, AD-85.[13] Used in its elastic range only.

$\rho_0 = 3.435$ $Y_0 = 38$ kbar $G = 830$ kbar

$\sigma = 1.54\,\mu$

11. Gauge, Mica, clear muscovite[21-23]

$\rho_0 = 2.87$ $Y_0 = 0$ $G = 0$

$\sigma = 0.427\,\mu + 0.72\,\mu^2 + 1.5\,\mu^3 + 1.13\,E$

Kapton and/or Epoxy[15]

$$\rho_0 = \frac{1.19\,t_\ell + 1.44\,t_k}{t}$$ $Y_0 = 0$ $G = 0$

t = total thickness of gauge

t_ℓ = thickness of epoxy

t_k = thickness of Kapton

$\sigma = 0.0884\,\mu + 0.101\,\mu^2 + 0.226\,\mu^3 + 1.13\,E$

50/50 Mix of Mica and Epoxy[21-23]

$\rho_0 = 2.0$ $Y_0 = 0$ $G = 0$

$P = 0.162\,\mu + 0.234\,\mu^2 + 0.745\,\mu^3 + 1.2\,E$

ACKNOWLEDGMENTS

It is a pleasure to thank A. B. Copeland, who performed many of the experiments, V. W. Morasch, who made most of the gauges, and A. E. Abey, who made the static measurements.

REFERENCES

*This work was performed under the auspices of the United States Atomic Energy Commission.

1. P. J. A. Fuller and J. H. Price, Nature (Jan. 20, 1962).
2. D. D. Keough and J. Y. Wong, J. Appl. Phys. 41, 3 (1970).
3. E. Barsis, E. Williams, and C. Skoog, J. Appl. Phys. 41, 13 (1970).
4. M. L. Wilkins, Methods in Computational Physics (Academic Press, N. Y., 1964) Vol. 3, p. 211.
5. V. M. Zaitsev, P. F. Pokhi, and K. K. Shvedov, Dakl. Akad. Nauk SSSR 132, 1339 (1960).
6. Reference to a company or product name does not imply approval or recommendation of the product by the University of California or the U. S. Atomic Energy Commission to the exclusion of others that may be suitable.
7. Clear Moscovite Mica, Spruce Pine Mica Co., Spruce Pine, N. C.
8. Trade name: Polyimide Film, E. E. DuPont de Nemours & Co.
9. 828 Epon, Shell Oil Company.
10. S. Thunborg, G. E. Ingram, and R. A. Graham, Rev. Sci. Instrum. 35, 1 (1964).
11. L. V. Al'tshuler, Usp. Fiz. Nauk 85, 197-258 (1965).
12. J. T. Rosenberg, M. J. Ginsberg, and R. F. Williams, Bull. Am. Phys. Soc., Ser. II, 17, 11 (1972).
13. W. H. Gust and E. B. Royce, J. Appl. Phys. 42, 1 (1971).
14. G. R. Fowles, J. Appl. Phys. 32, 8 (1961).

15. M. H. Rice, R. G. McQueen, and J. M. Walsh, Solid State Physics (Academic Press, N. Y., 1958) Vol. 6, p. 12.
16. C. D. Lundergan, The Hugoniot Equation of State of 6061-T6 Aluminum at Low Pressures, Sandia Laboratories, Albuquerque, N. Mex., Rept. SC-4637(RR) (1961).
17. J. W. Taylor, Uranium Shock Properties, Los Alamos Scientific Laboratory, Rept. LADC-5626 (1963).
18. L. M. Barker and R. E. Hollenback, J. Appl. Phys., 41, 4208 (1970).
19. D. R. Christman, W. M. Isbell, and S. G. Babcock, Measurement of Dynamic Properties of Materials—Copper, MSL-70-23 (Defense Atomic Support Agency 2501-1) (1971) Vol. V.
20. J. Wolfe, Coordinating ed., Aerospace Structural Metals Handbook, AFML-TR-68-115 (Mechanical Properties Data Center, Belfour Stulen, Inc., Traverse City, Mich., 1972) Vol. 3, Code 3601, p. 1.
21. L. H. Adams and J. Williamson, Franklin Inst., 195, 475 (1923).
22. Alexandrov and Rychova, Bull. (Izvestiya) of Acad. Sci. USSR, Geophys. Ser. 12, 1165 (1961).
23. F. Birch, in Handbook of Physical Constants, S. P. Clark, Jr., ed. (The Geological Soc. of Amer., Memoir 97, 1966) p. 97.

Table I. Manganin maximum stress calibration.

Shot I.D.	Material[a]	Velocity mm/μsec	Stress kbar	Insulator K-Kapton M-Mica	Gauge total thickness mils	Gauge resistance change $\Delta R/R_0$		
						Gauge 1	Gauge 2	Average
3177	Al 6061-T6	0.281	22	K	3	0.057	0.058	0.058
3238	Diamonite	0.136	23	K	4	0.062	0.061	0.062
3196	Sapphire	0.113	25	K	3	0.066	0.070	0.068
3224	Silica	0.502	30	K	3	0.085	0.081	0.083
9667	Al 2024-T4	0.591	47	M	5	0.129	0.129	0.129
9666	Al 2024-T4	0.618	49	M	5	0.148	0.149	0.149
9668	Al 2024-T4	0.629	50	M	5	0.139	0.142	0.141
1130	Diamonite	0.288	53	K	3	0.138	0.140	0.139
3190	Uranium	0.200	55	K	3	0.150	0.144	0.147
3188	Uranium	0.203	56	K	3	0.153	0.149	0.151
3114	Al 2024-T4	0.705	57	M	5	0.160	0.164	0.162
3116	Al 2024-T4	0.718	58	M	5	0.164	0.167	0.166
1114	Al 6061-T6	0.794	62	K	3	0.169	0.165	0.167
1111	Al 6061-T6	0.802	63	K	3	0.170	0.174	0.172
3200	Al 6061-T6	0.809	65	K	3	0.178	0.181	0.180
3201	Al 6061-T6	0.811	66	K	3	0.180	0.183	0.182
1142	Diamonite	0.356	66	K	3	0.169	0.176	0.173
3195	Sapphire	0.318	72	K	3	0.195	0.200	0.197
297	Al 6061-T6	0.946	79	M	5	0.208	0.212	0.210
3141	Al 2024-T4	1.200	103	M	5	0.281	—	0.281
3143	Al 2024-T4	1.211	103	M	6	0.285	—	0.285
3184	Uranium	0.372	106	K	3	0.297	0.273	0.285
3155	Al 2024-T4	1.247	107	M	6	0.321	—	0.321
298	Al 6061-T6	1.372	119	M	6	0.313	—	0.313
3156	Al 2024-T4	1.595	142	M	7	0.387	—	0.387
3157	Al 2024-T4	1.607	143	M	6	0.425	—	0.425
299	Al 6061-T6	1.861	170	M	6	0.447	—	0.453
366	Al 6061-T6	1.871	172	M	6	0.422	0.423	0.423
301	Al 6061-T6	1.874	172	M	6	0.457	0.459	0.458
300	Al 6061-T6	2.562	247	M	6	0.648	0.652	0.650
1137	Uranium	0.943	287	M	6	0.735	0.739	0.737
1136	Uranium	0.945	288	K	3	0.721	0.722	0.722
363	Cu OFHC	1.649	380	M	6	0.916	0.918	0.917
302	Cu OFHC	1.691	392	M	6	0.97	0.99	0.98
365	Cu OFHC	1.703	396	M	6	0.945	1.021	0.98
368	Cu OFHC	1.761	411	M	6	1.01	1.07	1.04

[a]Material equations of state are found in Appendix A. Shot 3238 used an AD-85 alumina flyer with a Diamonite target. In each other shot, target and flyer were of the same material.

Table II. Manganin dynamic hysteresis.

shot No.	Geometry[a] Flyer Materials (Ref.) Thickness (cm)	Geometry[a] Target[c] Materials (Ref.) Thickness (cm)	Velocity mm/μsec	Stress, maximum σ_1 kbar	Initial gauge resistance R_0 ohm	Gauge resistance at maximum stress R_1 ohm	Gauge resistances at unloading stresses R ohm	Calculated[b] unloading stresses from gauge data σ kbar	Unloading stresses from shot parameters kbar	Error %
3226	Al_2O_3[1] (0.344)	PMMA[8] PMMA[8] (0.313) (1.275)	0.817	31	9.75	10.65	10.40	21.3	21.2	+0.5
							10.24	15	15.4	-2.6
							10.14	11.1	11.6	-4.5
							10.08	8.8	9	-2.3
							10.04	7.2	7.3	-1.4
3224	PMMA[8] SiO_2[9] (1.000) (0.297)	SiO_2[9] SiO_2[9] (0.186) (0.590)	0.502	30	11.27	12.21	11.78	15	14	+6.7
3200	Al^3 PMMA[8] Al^3 (1.000) (0.150) (0.158)	Al^3 Al^3 (0.307) (1.000)	0.809	65	7.57	8.99	8.23	27	26.6	+1.5
3201	Al^3 (0.652)	Al^3 Al^3 (0.635) (1.270)	0.811	66	7.60	8.96	7.70	2	0	
3236	Cu[6] U[4] (1.00) (0.1033)	Al_2O_3[5] Al_2O_3[5] (0.3189) (1.2705)	0.317	78.5	9.856	12.03	11.74	67.3	66	+1.9
							9.98	-1.3		
3155	Al^2 (1.270)	Al^2 Al^2 MG[7] (0.800) (0.800) (2.000)	1.247	107	9.38	12.28	11.55	77.4	75	+3.2
S300	Zelux[8] Al^3 (1.000) (0.300)	Al^3 Al^3 (0.559) (0.775)	2.562	247	7.64	12.51	10.02	123	120	+2.4

[a]Material equations of state are listed in Appendix A.

[b]$\sigma = \sigma_1 - 0.38\ [(R_1 - R)/R_0]$.

[c]Gauges were of 1 mil wire insulated with 1 mil kapton in shots 3226, 3224, 3200, 3201, 3236; 1 mil mica was used in shots 3155 and S300. Gauges were placed between the first two plates of the target.

FIGURE CAPTIONS

Fig. 1 Gun-accelerated flyer impact geometry.

Fig. 2 Manganin gauge circuit.

Fig. 3 Static and dynamic calibration of 1 mil Manganin wire.

Fig. 4 Shot 3226 X-T diagram illustrating the wave reflections in the flyer that cause the stepped release at the gauge location. The target is made thick enough so that a rarefaction from its free surface arrives at the gauge much later in time.

Fig. 5 Shot 3227 stepped release. Particle velocity, dotted line; machine calculation, solid line.

Fig. 6 Shot 3226 stepped release. Manganin hysteresis, dotted line; machine calculation, solid line.

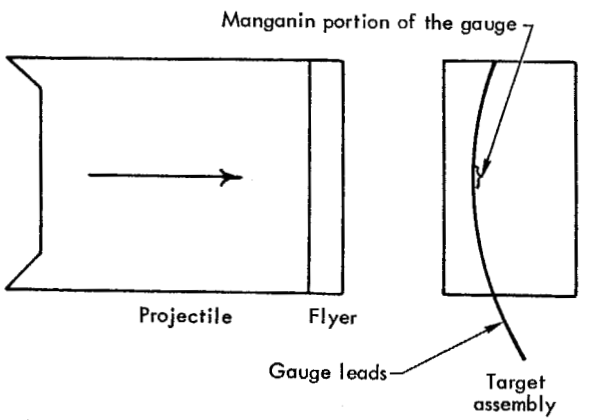

Lyle - Fig. 1

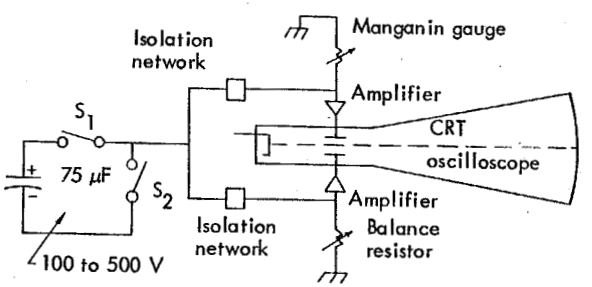

Lyle - Fig. 2

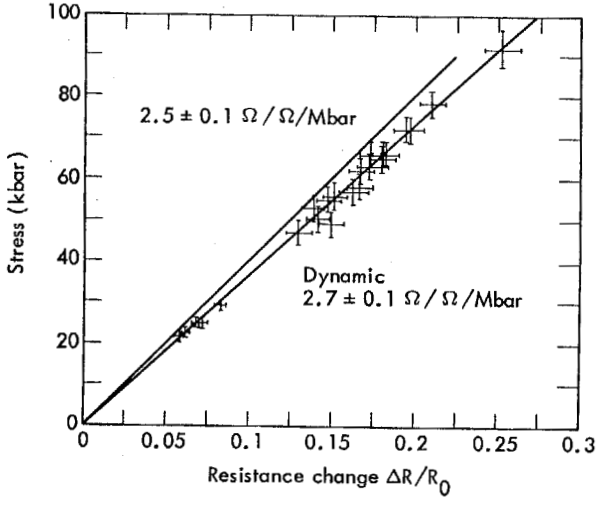

Lyle - Fig. 3

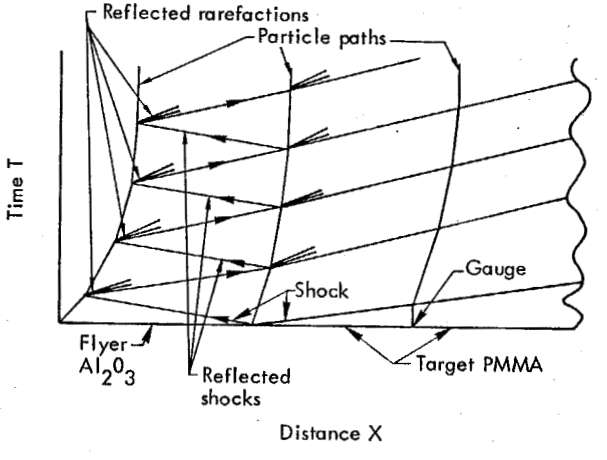

Lyle - Fig. 4

Fig 3 74664 SR

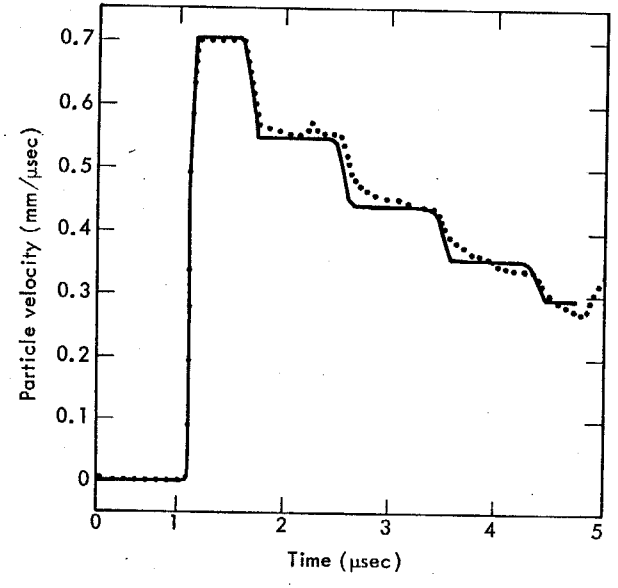

Lyle - Fig. 5

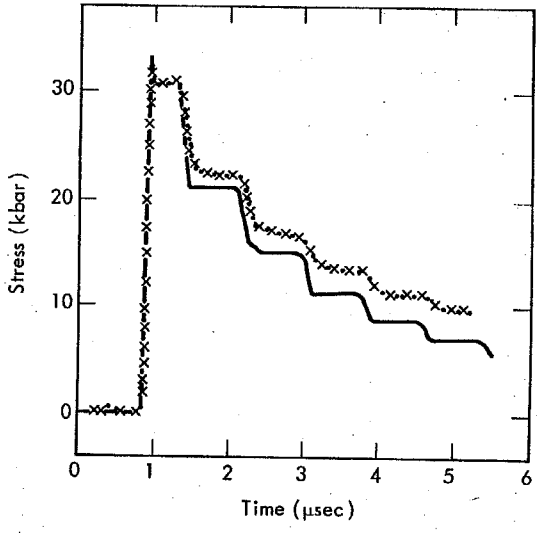

Lyle - Fig. 6

DISTRIBUTION

LLL Internal Distribution

Roger E. Batzel	
H. L. Reynolds	
R. L. Wagner	
M. L. Wilkins	
F. S. Eby	
G. A. Broadman	
G. T. Longerbeam	
J. W. Lyle	15
D. L. Banner	5
R. L. Brier	5
LBL Library	
TID File	30

RBC/rt